Dynamics of liquid N_2 studied by neutron inelastic scattering

Karen Schou Pedersen*
Department of Physics, University of Edinburgh, Edinburgh, Scotland

Kim Carneiro
Physics Laboratory I, Universitetsparken 5, DK-2100 København Ø and Risø National Laboratory, DK-4000 Roskilde, Denmark

Flemming Yssing Hansen
Fysisk-Kemisk Institut, The Technical University of Denmark, DK-2800 Lyngby, Denmark
(Received 10 August 1981)

Neutron inelastic-scattering data from liquid N_2 at wave-vector transfers κ between 0.18 and 2.1 Å^{-1} and temperatures ranging from $T=65-77$ K are presented. The data are corrected for the contribution from multiple scattering and incoherent scattering. The resulting dynamic structure factor $S(\kappa,\omega)$ is compared with $S(\kappa,\omega)$ determined by a molecular-dynamics calculation and with that calculated from a linearized Vlasov equation. For $\kappa \leq 0.3$ Å^{-1} the experimental $S(\kappa,\omega)$ is compared with the values predicted by hydrodynamic theory.

I. INTRODUCTION

Being a homonuclear diatomic liquid, the condensed phase of N_2 is one of the simplest liquids presenting rotational degrees of freedom. As such, considerable interest has been devoted to this liquid. Studies of the molecular structure have been made by Dore *et al.*[1] and by Pedersen *et al.*[2] using neutron diffraction. The microscopic dynamics has been investigated by Carneiro *et al.*[3] using neutron inelastic scattering, as well as by Weis *et al.*[4] performing a molecular-dynamics (MD) simulation. The dynamic structure factor, $S(\kappa,\omega)$, agrees fairly well in these two studies at larger wave vectors ($\kappa \gtrsim 1.7$ Å^{-1}), but at smaller wave vectors there are larger discrepancies between the neutron-scattering results and the MD results. These discrepancies were, in Ref. 4, inferred to stem from lack of correction for multiple scattering. In order to derive more accurate values for $S(\kappa,\omega)$ of liquid N_2 at smaller wave vectors, we have performed neutron inelastic-scattering experiments at wave-vector transfers κ between 0.18 and 2.1 Å^{-1} and temperatures ranging from $T=65$ to 77 K. The data have been corrected for multiple scattering using the method of Copley[5] and a comparison is made between this method and that of Sears.[6] We also show that in order to derive accurate values for $S(\kappa,\omega)$ at the smaller wave vectors, one must subtract the incoherent scattering from the measured intensities. The measurements have preferably been performed at wave vectors and temperatures such that the MD simulations could be compared directly with our results.

II. BASIC FORMULAS

The sample dynamics is related to the neutron-scattering properties via the double differential scattering cross section

$$\frac{d^2\sigma}{d\Omega\, d\omega}=\frac{N}{4\pi}\frac{|\vec{k}|}{|\vec{k}_0|}[\sigma_{\rm coh}S(\vec{\kappa},\omega)+\sigma_{\rm inc}S_{\rm inc}(\vec{\kappa},\omega)]\ , \tag{1}$$

where N is the number of scattering nuclei, $\vec{k}_0$ and $\vec{k}$ are the incoming and outgoing wave vectors of the neutron, which are related to the wave vector $\vec{\kappa}$, and the energy $\hbar\omega$, transferred to the system by a neutron through the relations $\vec{\kappa}=\vec{k}_0-\vec{k}$ and $\hbar\omega=\hbar^2(k_0^2-k^2)/2m_n$, where m_n is the neutron mass. $\sigma_{\rm coh}$ and $\sigma_{\rm inc}$ are the coherent and incoherent neutron-scattering cross sections. Since in isotropic systems such as liquids only the length of the scattering vector is of importance, we use κ

here. The two dynamic structure factors, $S(\kappa,\omega)$ and $S_{\rm inc}(\kappa,\omega)$, both obey the principle of detailed balance

$$S(\kappa,\omega)=e^{\hbar\omega/k_BT}S(-\kappa,-\omega)\ , \tag{2}$$

where k_B is the Boltzmann constant. It is convenient to represent the experimental data in the form of the symmetrized dynamic structure factor

$$\tilde{S}(\kappa,\omega)=e^{-\hbar\omega/2k_BT}S(\kappa,\omega)\ . \tag{3}$$

When comparing to classical theories such as molecular dynamics or hydrodynamics, $\tilde{S}(\kappa,\omega)$ is used since it corrects for quantum effects to first order $\hbar$.[7] The static structure factor, $S(\kappa)$, equals the zeroth moment of the coherent dynamic structure factor

$$\int_{-\infty}^{\infty}S(\kappa,\omega)d\omega=S(\kappa)\ , \tag{4}$$

while the zeroth moment of the incoherent scattering function equals unity:

$$\int_{-\infty}^{\infty}S_{\rm inc}(\kappa,\omega)d\omega=1\ . \tag{5}$$

The expression for the first energy moment, first obtained by Placzek,[8] takes the form

$$\int_{-\infty}^{\infty}\omega S(\kappa,\omega)\,d\omega=\frac{\kappa^2}{2M}\ , \tag{6}$$

where M is the effective mass of the scatterer. For the second energy moment de Gennes[9] derived the following approximate result for a diatomic homonuclear liquid:

$$\int_{-\infty}^{\infty}\omega^2\tilde{S}(\kappa,\omega)\,d\omega=\frac{\kappa^2}{M_a}\frac{k_BT}{S(\kappa)}[\tfrac{5}{6}+m(\xi)]\ , \tag{7}$$

where d is the molecular bond length, $\xi=\kappa d$,

$$m(\xi)=\frac{1}{2\xi^3}[2\xi\cos\xi+(\xi^2-2)\sin\xi]\ ,$$

and M_a the atomic mass.

III. EXPERIMENTAL

The experiments were performed as constant κ scans using triple-axis spectrometers at Risø National Laboratory. A summary of the experiments is given in Table I. Experiment IV ($\kappa=2.3$ Å^{-1} and 4 Å^{-1}) was only made to get data for the multiple-scattering correction and will not be analyzed any further. All the other experiments were performed at the cold source using the triple-axis spectrometer TAS I. Pyrolytic graphite (PG) crystals were used as monochromators and analyzers. Higher-order reflections were removed

TABLE I. Summary of neutron inelastic-scattering experiments on liquid N_2.

Experiment No.	Wave-vector transfer κ (Å^{-1})	Energy transfer $\hbar\omega$ (meV) 5-meV incident energy	Energy transfer $\hbar\omega$ (meV) 14-meV incident energy	Temperature (K)
II	0.18	−2.1→1.05	−1.9→1.8	65,74,76
	0.22	−1.5→1.3	−2.4→2.2	
	0.26	−1.8→1.5	−2.9→2.6	
	0.30	−2.1→1.6	−3.3→3.0	
I	0.30	−2.1→1.6	−3.3→3.0	72
	0.45	−3.0→2.0	−5.0→4.4	
	0.75	−3.0→2.0	−9.2→6.8	
	1.05	−3.0→2.0	−10.0→7.0	
	1.40	−3.0→2.0	−10.0→7.0	
	1.90	−3.0→2.0	−10.0→7.0	
III	1.70	−3.0→2.0	−10.0→7.0	66,74,77
	1.90	−3.0→2.0	−10.0→7.0	
	2.10	−3.0→2.0	−10.0→7.0	
IV	2.30	−3.0→0.0	−10.0→7.0	72
	4.00		−10.0→0.0	

by a cooled Be crystal filter in case of 5-meV incident energy and a PG filter in case of 14-meV incident energy. The sample chamber consisted of an aluminium cylinder with an inner radius of 0.9 cm and a wall thickness of 1 mm. To reduce the multiple scattering it was divided into smaller chambers by parallel horizontal plates at intervals of 0.45 cm. The energy resolution width (FWHM) was 0.17 meV for the 5-meV incident energy and 0.93 meV for the 14-meV incident energy. As an example the measured intensity data for $\kappa=1.9$ Å^{-1} and $T=66$ K, $T=74$ and 77 K are shown in Fig. 1 together with the data for the empty Al cylinder.

IV. DATA CORRECTIONS

A. Instrumental corrections

The data of each of the scans in Table I were corrected for the scattering from the empty cylinder and for instrumental sensitivity.[10] The instrumental energy resolution width is lower for the 5-meV incident energy data, while on the other hand the higher energy transfers are only reached by the 14-meV incident energy neutrons. Since the resolution is most important for the ω values close to zero where $S(\kappa,\omega)$ may vary considerably with ω, the 5-meV incident energy data are used for $|\hbar\omega|<1-2$ meV, the exact value depending on the wave-vector transfer, and the 14-meV data for higher energy transfers. Both coherent and incoherent as well as multiple scattering fulfill the principle of detailed balance as given by Eq. (2). Therefore, when $I(\kappa,\omega)$ represents the background and sensitivity corrected scattering intensity, the function

$$\tilde{I}(\kappa,\omega)=e^{-\hbar\omega/2k_BT}I(\kappa,\omega) \tag{8}$$

should be symmetric in ω. Figure 2 compares $\tilde{I}(\kappa,\omega)$ for positive and negative energy transfers at $\kappa=1.9$ Å^{-1} and $T=72$ K. The data for $\omega>0$ are generally slightly higher than those for $\omega<0$, but the difference is considered small enough to be neglected and the average values of $\tilde{I}(\kappa,\omega)$ for positive and negative energy transfers are used.

In principle our data should also be corrected for the finite instrumental κ and ω resolution, and this correction was made in the study of liquid Ar by Sköld *et al.*[11] We have approached this problem differently by using sufficient high resolution when necessary. Since all measured energy widths are broader than 0.9 meV (FWHM), i.e., much larger than the instrumental resolution of 0.17 meV for 5-meV neutrons, our $S(\kappa,\omega)$ is not significantly affected by energy resolution. On the other hand, the wave-vector resolution plays a role very close to $\kappa=0$, and this probably influences our $S(\kappa,\omega)$ at the smallest wave vectors (experiment II). At larger κ's the effect of wave-vector resolution is negligible.

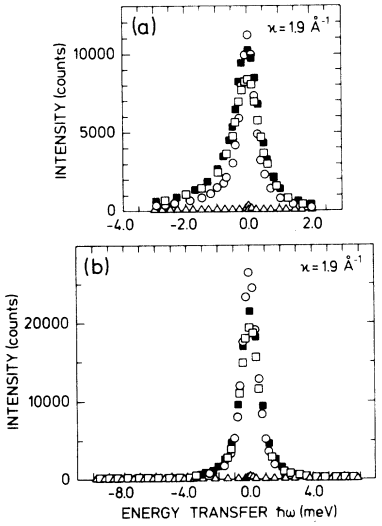

FIG. 1. Measured intensity data from the empty cell (Δ) and from the cell filled with liquid N_2 for $\kappa=1.9$ Å^{-1} and $T=65$ K (●), $T=74$ K (■), and $T=77$ K (□). (a) 5-meV incident energy. (b) 13.7-meV incident energy.

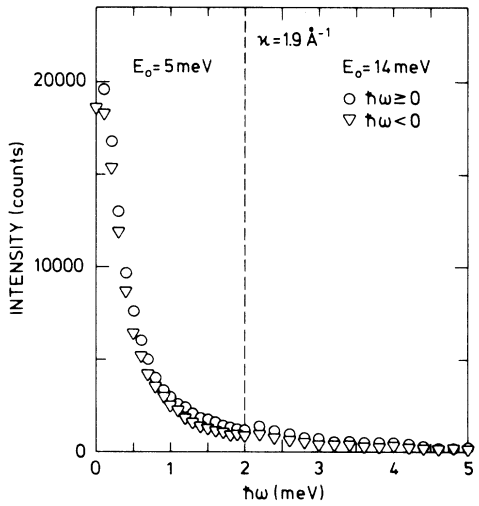

FIG. 2. Symmetrized scattering law for liquid N_2 at $\kappa=1.9$ Å^{-1}, to test the intensity corrections for the triple-axis spectrometer. The dashed line indicates the energy transfer below which the $E_0=5$-meV data are used and above which the $E_0=14$-meV data are used.

B. Multiple-scattering correction

The available computer programs for multiple-scattering correction requires some knowledge of the dynamic structure factor, $S(\kappa,\omega)$. This problem is bypassed if one assumes $S(\kappa,\omega)$ from theory or MD,[11,12] but this is not fully satisfactory if one wants to derive a truly experimental dynamic structure factor. We have derived $S(\kappa,\omega)$ without any assumptions about the shape in the wave-vector region $0.30\ \text{Å}^{-1} \leq \kappa \leq 4.0\ \text{Å}^{-1}$; namely, by performing the multiple-scattering calculation as a self-consistent correction procedure using the Monte Carlo simulation program of Copley.[5] In the mentioned interval the data of experiment I, III, and IV [corrected as described above and normalized to the tabulated values of $S(\kappa)$[13] at the appropriate temperature] were used as a first estimate of $S(\kappa,\omega)$. For κ and ω values between those covered by measurements, $S(\kappa,\omega)$ is found by interpolation in (κ,ω), while it is set to zero outside the measured ω interval. For $\kappa < 0.3\ \text{Å}^{-1}$ a hydrodynamic model is used[14]:

$$\tilde{S}(\kappa,\omega)=\frac{1}{2\pi}S(\kappa)\left[\frac{\gamma-1}{\gamma}\frac{2D_T\kappa^2}{\omega^2+(D_T\kappa^2)^2}+\frac{1}{\gamma}\left[\frac{\Gamma\kappa^2}{(\omega+c_s\kappa^2)^2+(\Gamma\kappa^2)^2}+\frac{\Gamma\kappa^2}{(\omega-c_s\kappa^2)^2+(\Gamma\kappa^2)^2}\right]\right], \tag{9}$$

where γ is equal to the ratio between the specific heat at constant pressure $C_p = 4.07\times10^3$ J/kg K and the specific heat at constant volume $C_v = 2.23\times10^3$ J/kg K. The thermal diffusivity $D_T = \lambda/\rho C_v\gamma$, where $\lambda = 0.149$ J/ms K is the thermal conductivity and $\rho = 804$ kg/m^3 is the density. The sound attenuation coefficient

$$\Gamma=\tfrac{1}{2}\left[\frac{\lambda(\gamma-1)}{\rho C_v\gamma}+\frac{4/3\eta+\zeta}{\rho}\right],$$

where $\eta = 2.07\times10^{-4}$ kg/ms is the shear viscosity and $\zeta = 2.47\times10^{-5}$ kg/ms the bulk viscosity. The velocity of sound $c_s = 914$ m/s. The above values for C_p, C_v, λ, η, ζ, and c_s are from Ref. 15 and at $T = 72$ K. The value of the static structure factor, $S(\kappa)$, may be calculated independently in the so-called compressibility limit:

$$S(\kappa)=\rho k_B T\chi \quad \text{when } \kappa\to0\ , \tag{10}$$

where ρ is the number density and $\chi = M/(\rho c_s^2)$ is the isothermal compressibility.

For $\kappa > 4\ \text{Å}^{-1}$, a free-particle model is used[16]:

$$\tilde{S}(\kappa,\omega)=\left[\frac{M}{2\pi k_B T\hbar^2\kappa^2}\right]^{1/2}\times\exp\left[-\frac{M}{2k_B T\hbar^2\kappa^2}\left[\hbar\omega-\frac{\hbar^2\kappa^2}{2M}\right]^2\right]. \tag{11}$$

The effective mass of a N_2 molecule is set to $16.8m_n$.[17,18] After each run of the multiple-scattering program, the input data for $S(\kappa,\omega)$ were corrected accordingly, and the runs were continued until the corrected data and the latest input data were identical.

The second and following runs of the multiple-scattering computer program only cause minor changes in the dynamic structure factors but for $\kappa \leq 0.75\ \text{Å}^{-1}$ a perfect consistency is not obtained until after 4–5 complete runs. The final multiple-scattering corrected data were obtained by performing two additional runs using a slightly different normalization procedure. The intensity data for $\kappa = 1.9\ \text{Å}^{-1}$ corrected for the multiple-scattering contribution as described above were at each step of this procedure renormalized to the tabulated value of $S(\kappa)$. The preliminary corrected data for the other wave-vector transfers were then normalized using the normalization constant found for $\kappa = 1.9\ \text{Å}^{-1}$. The idea behind this is that at $\kappa = 1.9\ \text{Å}^{-1}$, $S(\kappa)$ is well determined and the relative contribution to the scattering intensity from multiple and incoherent scattering is small, which means that the normalization constant can be determined with high accuracy. This $S(\kappa,\omega)$ was used in a comparison between the multiple scattering calculated by the Monte Carlo method and by the Sears method. The results are shown in Table II. Since the Sears method is much more expensive in computer time than the Monte Carlo method, we have only made a comparison between the two methods for 5-meV neutrons. From Table II is seen that one generally finds a higher multiple-scattering contribution by the Sears method than by the Monte Carlo method. For wave-vector transfers where $S(\kappa)$ is small, minor

TABLE II. Summary of the multiple-scattering corrections of the neutron inelastic-scattering data on liquid N_2 at $T=72$ K.

	$E_0=5$ meV					$E_0=14$ meV		
		$I(\kappa)$-Mult. Scat. $\times 10^3$		Mult. Scat. in % of Total Scat.			$I(\kappa)$-Mult. Scat. $\times 10^3$	Mult. Scat. in % of Total Scat.
κ (Å^{-1})	$I(\kappa)$ $\times 10^3$	MC[a]	AM[b]	MC	AM	$I(\kappa)$ $\times 10^3$	(MC)	(MC)
0.30	2.24	0.853	0.624	62	72	3.38	1.72	49
0.45	2.93	1.11	0.827	62	72	4.08	1.91	53
0.75	2.72	1.20	0.783	56	71	4.71	2.38	49
1.05	2.78	1.76	1.40	37	50	5.23	3.39	35
1.40	3.39	2.93	2.73	14	20	8.06	6.69	17
1.90	22.1	21.5	20.8	2.7	5.9	42.7	41.1	3.7

[a]MC represents Monte Carlo.
[b]AM represents Analytical method.

differences in the calculated multiple scattering have a pronounced effect on the resulting $S(\kappa,\omega)$ as is apparent from Fig. 3, which for $\kappa=0.3$ Å^{-1} and an incident energy of 5 meV shows the results of both correction procedures. The reason for the discrepancy is probably the approximations introduced in the Sears method but has not been further analyzed. Since the Monte Carlo procedure is exact (neglecting numerical and statistical shortcomings, of course) and also because the computation is less, we have chosen to base our multiple-scattering correction entirely on the Monte Carlo method.

The scattering results for 0.18 Å$^{-1}\leq\kappa\leq$0.30 Å^{-1} and 1.7 Å$^{-1}\leq\kappa\leq$2.1 Å^{-1} and varying T were corrected for multiple scattering by the Monte Carlo method using the values of $S(\kappa,\omega)$ determined for $T=72$ K. The multiple scattering constitutes about 60% of the total scattering in the former κ interval and less than 10% in the latter one.

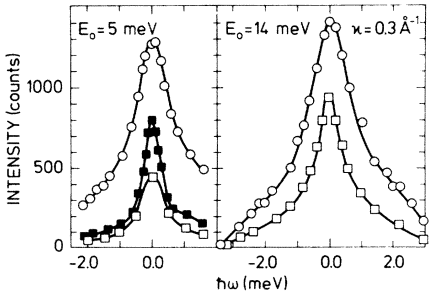

FIG. 3. Intensity data at $\kappa=0.3$ Å^{-1} before (●) and after multiple-scattering correction by Monte Carlo simulation (■), and using the analytical expression of Sears (□).

C. Corrections for incoherent scattering

Liquid N_2 is known to have a very small incoherent scattering cross section, but the tabulated value[19] of $\sigma_{inc}=0.3$ barn is subject to some uncertainty. An incoherent cross section would add extra intensity to $I(\kappa,\omega)$ centered in $\omega=0$ but in the liquid phase it can be difficult to distinguish it from the coherent contribution. To investigate the problem further, neutron inelastic scattering was performed on solid N_2 at $T\approx 32$ K for κ values of 0.30, 0.45, 0.75, and 1.05 Å^{-1}. In the solid phase coherent and incoherent scattering can easily be distinguished. Any incoherent contribution will appear as an elastic line, whereas the coherent scattering for the mentioned wave vectors will be purely inelastic. For all four wave-vector transfers sharp elastic peaks were observed, which demonstrates that N_2 does have a measurable incoherent cross section. The intensity from liquid N_2 corrected for background, sensitivity, and multiple scattering equals

$$I(\kappa,\omega)=\text{const}[\sigma_{coh}S(\kappa,\omega)+\sigma_{inc}S_{inc}(\kappa,\omega)]\ . \tag{12}$$

A simple self-diffusion model is used for the symmetrized incoherent dynamic structure factor

$$\tilde{S}_{\text{inc}}(\kappa,\omega)=\frac{1}{\pi}\frac{D\kappa^2}{\omega^2+(D\kappa^2)^2}\ , \tag{13}$$

where D is the self-diffusion coefficient. For small κ values $\tilde{S}_{\text{inc}}(\kappa,\omega)$ is sharply centered around $\omega=0$ and, as opposed to the above-mentioned treatment of $S(\kappa,\omega)$, it is therefore necessary to take into account the instrumental resolution:

$$I_{\text{inc}}(\kappa,\omega)=\text{const}\,\sigma_{\text{inc}} \times\int_{-\infty}^{\infty}R(\omega'-\omega)S_{\text{inc}}(\kappa,\omega')\,d\omega'\ , \tag{14}$$

where $I_{\text{inc}}(\kappa,\omega)$ is the incoherent contribution to the background subtracted and sensitivity corrected scattering intensity. It is assumed that the resolution function, R, has a Gaussian line shape

$$R(\omega)=\frac{1}{\sqrt{2\pi}\Delta}e^{-\omega^2/2\Delta^2}\ , \tag{15}$$

where $\hbar\Delta=0.072$ meV is the measured instrumental resolution width (corresponding to 0.17 meV FWHM). An independent evaluation of σ_{inc} is obtained by varying σ_{inc} and studying the resulting $I(\kappa,\omega)-I_{\text{inc}}(\kappa,\omega)$. At least at small κ's too high values of σ_{inc} will cause a local minimum in $\tilde{S}(\kappa,\omega)$ at $\omega=0$, while too small values will add an extra top to $\tilde{S}(\kappa,\omega)$ at $\omega\approx 0$. The self-diffusion coefficient for liquid N_2 at 72 K is set to 3.0×10^{-5} cm^2/s.[20] Figure 4 shows the dynamic structure factor before and after subtraction of the incoherent contribution for σ_{inc} values of 0.2, 0.3, and 0.4 barn. The tabulated value of $\sigma_{\text{inc}}=0.3$ barn gives the most reasonable line shape of $S(\kappa,\omega)$ and is therefore used here.

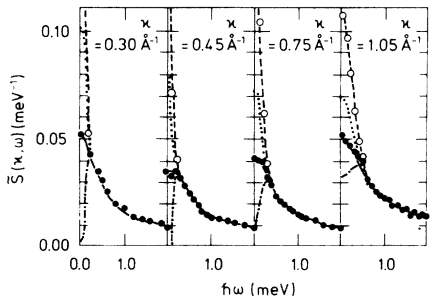

FIG. 4. Intensity data corrected for multiple scattering by the Monte Carlo method before (- - -) and after subtraction of the incoherent scattering contribution employing values of $\sigma_{\text{inc}}=0.2$ barn (· · · ·), $\sigma_{\text{inc}}=0.3$ barn (——), and $\sigma_{\text{inc}}=0.4$ barn (- · - · -).

V. RESULTS

A. $\tilde{S}(\kappa,\omega)$ and $S(\kappa)$

The symmetrized dynamic structure factors of liquid N_2, $\tilde{S}(\kappa,\omega)$, are tabulated in Tables III–V. Table III gives the structure factors for $\kappa\leq 0.30$ Å^{-1} and temperatures between 65 and 77 K, Table IV the structure factors for 0.30 Å$^{-1}\leq\kappa\leq 1.90$ Å^{-1} and $T=72$ K, and Table V the dynamic structure factors for 1.70 Å$^{-1}\leq\kappa\leq 2.10$ Å^{-1} and temperatures between 65 and 77 K. Since the resolution, in particular the wave-vector resolution coming from vertical collimation, becomes more important the smaller the κ values, and also because the multiple and incoherent scattering constitute a large part of the total scattering at small κ values, the data of Table III must be attributed less accuracy than those of Table IV and V. A graphical representation of the tabulated data for $T=72$ K is shown in Fig. 5.

Compared with the earlier neutron-scattering results of Carneiro and McTague,[3] our values of $S(\kappa,\omega)$ represent an appreciable improvement in accuracy. Firstly, since the multiple-scattering line shape is in general broader in ω than $S(\kappa,\omega)$, the wings of $S(\kappa,\omega)$ of Ref. 3 were overestimated, and, secondly, the incoherent scattering added a quasielastic contribution. Both these effects are strongest at low κ's, and this is indeed where the most remarkable differences between the MD results and those of Ref. 3 were found.

Relatively little has been done regarding the temperature dependence of the dynamics of liquids. Even our bare intensity data of Fig. 1 show, however, that there is an appreciable variation in $S(\kappa,\omega)$ of liquid N_2 with temperature. This temperature dependence of the dynamic structure factor is, however, confined to wave vectors around the peak in $S(\kappa)$, i.e., $\kappa\approx 2$ Å^{-1}, where for instance $S(\kappa,0)$ varies with 30% when T is raised from 64 to 76 K. Our results are shown in Fig. 6. $S(\kappa)$ varies 23% in this temperature region. As one would expect from the temperature dependence of the hydrodynamic parameters in (9), $S(\kappa,\omega)$ for small wave vectors (Table III) varies only a little. Figure 7 shows the static structure factor, $S(\kappa)$, of liquid N_2 at $T=72$ K obtained as

$$\int_{\Delta E_{\text{min}}/\hbar}^{\Delta E_{\text{max}}/\hbar}S(\kappa,\omega)d\omega$$

from the experimental dynamic structure factors and from the molecular-dynamics calculation compared with $S(\kappa)$ of Ref. 13. Also shown in Fig. 7

TABLE III. Dynamic structure factors, $\tilde{S}(\kappa,\omega)$, of liquid N_2 determined from neutron inelastic-scattering data for wave vectors 0.18 $Å^{-1} \leq \kappa \leq 0.30$ $Å^{-1}$ at different temperatures.

$\hbar\omega$	$\kappa=0.18$ $Å^{-1}$			$\kappa=0.22$ $Å^{-1}$			$\kappa=0.26$ $Å^{-1}$			$\kappa=0.30$ $Å^{-1}$		
(meV)	$T=65$ K	$T=74$ K	$T=76$ K	$T=65$ K	$T=74$ K	$T=76$ K	$T=65$ K	$T=74$ K	$T=76$ K	$T=65$ K	$T=74$ K	$T=76$ K
0.0	0.0287	0.0411	0.0617	0.0431	0.0371	0.0351	0.0462	0.0462	0.0388	0.0525	0.0505	0.0635
0.1	0.0276	0.0403	0.0549	0.0412	0.0357	0.0341	0.0447	0.0444	0.0374	0.0522	0.0490	0.0505
0.2	0.0266	0.0375	0.0350	0.0358	0.0324	0.0323	0.0401	0.0399	0.0331	0.0458	0.0452	0.0397
0.3	0.0254	0.0326	0.0294	0.0299	0.0289	0.0287	0.0333	0.0344	0.0297	0.0375	0.0335	0.0312
0.4	0.0246	0.0265	0.0240	0.0256	0.0251	0.0243	0.0279	0.0279	0.0240	0.0304	0.0301	0.0252
0.5	0.0202	0.0219	0.0218	0.0230	0.0228	0.0217	0.0234	0.0215	0.0204	0.0239	0.0226	0.0210
0.6	0.0149	0.0199	0.0192	0.0181	0.0191	0.0175	0.0186	0.0195	0.0181	0.0190	0.0193	0.0186
0.7	0.0153	0.0202	0.0181	0.0161	0.0175	0.0172	0.0158	0.0164	0.0159	0.0165	0.0170	0.0173
0.8	0.0127	0.0180	0.0165	0.0138	0.0145	0.0145	0.0144	0.0151	0.0153	0.0149	0.0146	0.0144
0.9	0.0108	0.0147	0.0139	0.0140	0.0142	0.0138	0.0124	0.0146	0.0140	0.0132	0.0137	0.0135
1.0	0.0096	0.0146	0.0142	0.0110	0.0130	0.0125	0.0120	0.0133	0.0125	0.0120	0.0128	0.0105
1.1	0.0087	0.0135	0.0120	0.0122	0.0121	0.0128	0.0110	0.0120	0.0115	0.0114	0.0124	0.0112
1.2	0.0091	0.0133	0.0114	0.0102	0.0122	0.0120	0.0101	0.0121	0.0120	0.0107	0.0117	0.0114
1.3		0.0131	0.0116		0.0104	0.0107	0.0083	0.0091	0.0102	0.0095	0.0106	0.0100
1.4	0.0094	0.0148	0.0109	0.0101	0.0110	0.0112	0.0084	0.0091	0.0086	0.0089	0.0100	0.0105
1.5		0.0103	0.0083		0.0110	0.0108		0.0099	0.0092	0.0090	0.0080	0.0089
1.6	0.0058	0.00106	0.0071	0.0095	0.0108	0.0108	0.0087	0.0087	0.0095	0.0074	0.0084	0.0081
1.7		0.0053			0.0087	0.0098		0.0100	0.0096	0.0070	0.0079	0.0076
1.8				0.0077	0.0067	0.0076	0.0085	0.0086	0.0093	0.0069	0.0074	0.0074
1.9					0.0078	0.0094		0.0089	0.0090		0.0080	0.0071
2.0				0.0086	0.0066	0.0094	0.0084	0.0087	0.0087	0.0078	0.0088	0.0074
2.1						0.0021		0.0075	0.0086		0.0084	0.0074
2.2						0.0004	0.0065	0.0077	0.0083	0.0072	0.0075	0.0073
2.3								0.0072	0.0075		0.0085	0.0074
2.4							0.0055	0.0058	0.0064	0.0081	0.0078	0.0077
2.5								0.0044	0.0068		0.0062	0.0070
2.6							0.0090		0.0011	0.0077	0.0078	0.0078
2.7											0.0072	0.0073
2.8										0.0085	0.0073	0.0088
2.9											0.0059	0.0070
3.0										0.0016	0.0011	0.0016

TABLE IV. Dynamic structure factors, $\tilde{S}(\kappa,\omega)$ of liquid N_2 at $T=72$ K determined from neutron inelastic-scattering data for 0.30 $\text{Å}^{-1} \leq \kappa \leq 1.90$ Å^{-1}.

ΔE (meV) \ κ (Å^{-1})	0.30	0.45	0.75	1.05	1.40	1.90
0.0	0.0524	0.0354	0.0412	0.0519	0.158	2.49
0.1		0.0335	0.0400	0.0492	0.151	2.54
0.2	0.0431	0.0352	0.0396	0.0470	0.143	2.14
0.3		0.0319	0.0318	0.0445	0.128	1.67
0.4	0.0346	0.0289	0.0283	0.0422	0.120	1.22
0.5	0.0309	0.0249	0.0233	0.0398	0.107	0.922
0.6	0.0253	0.0219	0.0205	0.0291	0.0785	0.721
0.7		0.0191	0.0197	0.0278	0.0729	0.602
0.8	0.0198	0.0163	0.0171	0.0248	0.0649	0.522
0.9		0.0145	0.0161	0.0237	0.0619	0.412
1.0	0.0178	0.0136	0.0149	0.0225	0.0662	0.355
1.1			0.0141	0.0217	0.0641	0.308
1.2	0.0131	0.0131	0.0132	0.0190	0.0584	0.269
1.3				0.0190	0.0592	0.232
1.4	0.0120	0.0117	0.0114	0.0169	0.0478	0.213
1.5				0.0170		0.201
1.6	0.0114	0.0107	0.00951	0.0137	0.0411	0.165
1.7				0.0156		0.161
1.8	0.0109	0.00992	0.00876	0.0135	0.0383	0.129
2.0	0.00860	0.00848	0.00869	0.0145	0.0365	0.109
2.2	0.00848	0.00916	0.00779	0.0137	0.0307	0.0764
2.4	0.00663	0.00881	0.00709	0.0136	0.0302	0.0616
2.6	0.00555	0.00835	0.00795	0.0113	0.0259	0.0526
2.8	0.00393	0.00824	0.00716	0.0110	0.0223	0.0462
3.0	0.00281	0.00734	0.00704	0.0110	0.0212	0.0384
3.2	0.00104	0.00803	0.00698	0.00972	0.0209	0.0332
3.4	0.00040	0.00717	0.00791	0.0107	0.0201	0.0301
3.6		0.00588	0.00677	0.00992	0.0167	0.0277
3.8		0.00503	0.00719	0.0105	0.0169	0.0238
4.0		0.00478	0.00596	0.0101	0.0155	0.0207
4.2		0.00248	0.00629	0.00836	0.0137	0.0165
4.4		0.00150	0.00647	0.00865	0.0105	0.0180
4.6		0.00190	0.00647	0.00910	0.0115	0.0161
4.8		0.00096	0.00650	0.00930	0.0107	0.0160
5.0		0.00062	0.00645	0.00662	0.00895	0.0136
5.2			0.00734	0.00836	0.0109	0.0129
5.4			0.00651	0.00684	0.0100	0.0121
5.6			0.00583	0.00697	0.00982	0.0109
5.8			0.00487	0.00673	0.00868	0.0124
6.0			0.00561	0.00510	0.00796	0.0101
6.2			0.00374	0.00649	0.00648	0.0111
6.4			0.00413	0.00537	0.00617	0.00980
6.6			0.00349	0.00603	0.00728	0.00876
6.8			0.00311	0.00707	0.00732	0.00832
7.0			0.00353	0.00657	0.00635	0.00734
7.2			0.00345	0.00473	0.00502	0.00646
7.4			0.00303	0.00487	0.00477	0.00602
7.6			0.00305	0.00491	0.00383	0.00541
7.8			0.00218	0.00407	0.00456	0.00614
8.0			0.00200	0.00310	0.00429	0.00429

TABLE IV. (*Continued.*)

ΔE (meV) \ κ (Å^{-1})	0.30	0.45	0.75	1.05	1.40	1.90
8.2			0.00242	0.00303	0.00433	0.00464
8.4			0.00174	0.00304	0.00273	0.00324
8.6			0.00072	0.00266	0.00256	0.00378
8.8			0.00083	0.00270	0.00228	0.00321
9.0			0.00063	0.00178	0.00249	0.00324
9.2			0.00053	0.00211	0.00180	0.00263
9.4				0.00138	0.00159	0.00297
9.6				0.00075	0.00150	0.00333
9.8				0.00021	0.00108	0.00259
10.0				0.00015	0.00098	0.00175

TABLE V. Dynamic structure factor, $\tilde{S}(\kappa,\omega)$ of liquid N_2 determined from neutron inelastic-scattering data for 1.70 Å$^{-1} \leq \kappa \leq 2.1$ Å^{-1} at different temperatures.

$\hbar\omega$	$\kappa=1.70$ Å^{-1}			$\kappa=1.90$ Å^{-1}			$\kappa=2.10$ Å^{-1}		
(meV)	$T=66$ K	$T=74$ K	$T=77$ K	$T=66$ K	$T=74$ K	$T=77$ K	$T=66$ K	$T=74$ K	$T=77$ K
0.0	0.802	0.950	1.01	2.82	2.23	2.03	1.00	0.588	0.611
0.1	0.813	1.02	1.07	2.57	2.23	2.08	0.949	0.571	0.567
0.2	0.788	1.00	1.06	1.99	2.05	1.91	0.903	0.557	0.567
0.3	0.654	0.857	0.945	1.40	1.72	1.66	0.754	0.510	0.533
0.4	0.513	0.717	0.799	0.965	1.33	1.34	0.613	0.455	0.489
0.5	0.410	0.598	0.659	0.691	1.09	1.09	0.417	0.416	0.444
0.6	0.344	0.495	0.584	0.533	0.863	0.911	0.391	0.388	0.419
0.7	0.281	0.425	0.519	0.439	0.725	0.742	0.342	0.366	0.393
0.8	0.248	0.374	0.461	0.356	0.625	0.691	0.271	0.306	0.375
0.9	0.212	0.324	0.405	0.310	0.512	0.603	0.243		
1.0	0.193	0.278	0.348	0.274	0.436	0.514	0.208	0.256	0.258
1.1	0.176	0.254	0.308	0.259	0.372	0.440			0.207
1.2	0.163	0.218	0.269	0.243	0.328	0.366	0.200	0.206	
1.3	0.147	0.185	0.232		0.286	0.326			0.192
1.4	0.131	0.163	0.196	0.199	0.250	0.287	0.157	0.157	0.168
1.5		0.153	0.177		0.217	0.241			0.150
1.6	0.101	0.121	0.157	0.140	0.174	0.196	0.113	0.120	0.138
1.8	0.0805	0.0964	0.121	0.106	0.142	0.159	0.0928	0.102	0.124
2.0	0.0653	0.0786	0.0959	0.0903	0.112	0.115	0.0865	0.0939	0.109
2.2	0.0582	0.0645	0.0804	0.0715	0.0826	0.0959	0.0757	0.0845	0.0963
2.4	0.0494	0.0535	0.0632	0.0596	0.0657	0.0757	0.0637	0.0696	0.0835
2.6	0.0418	0.0466	0.0548	0.0481	0.0541	0.0658	0.0588	0.0643	0.0722
2.8	0.0368	0.0414	0.0457	0.0435	0.0468	0.0560	0.0499	0.0493	0.0608
3.0	0.0317	0.0323	0.0382	0.0389	0.0393	0.0465	0.0467	0.0548	0.0576
3.2	0.0270	0.0320	0.0330	0.0322	0.0370	0.0399	0.0422	0.0460	0.0543
3.4	0.0249	0.0283	0.0282	0.0276	0.0335	0.0348	0.0371	0.0403	0.0467
3.6	0.0223	0.0240	0.0253	0.0249	0.0271	0.0296	0.0320	0.0354	0.0390
3.8	0.0209	0.0226	0.0231	0.0217	0.0226	0.0266	0.0301	0.0305	0.0467
4.0	0.0171	0.0190	0.0193	0.0204	0.0207	0.0234	0.0255	0.0302	0.0337
4.2	0.0170	0.0165	0.0175	0.0181	0.0181	0.0214	0.0258	0.0257	0.0302
4.4	0.0142	0.0165	0.0166	0.0165	0.0166	0.0193	0.0198	0.0206	0.0267

TABLE V. (*Continued.*)

$\hbar\omega$ (meV)	$\kappa=1.70$ Å^{-1} $T=66$ K	$T=74$ K	$T=77$ K	$\kappa=1.90$ Å^{-1} $T=66$ K	$T=74$ K	$T=77$ K	$\kappa=2.10$ Å^{-1} $T=66$ K	$T=74$ K	$T=77$ K
4.6	0.0158	0.0150	0.0161	0.0162	0.0173	0.0181	0.0196	0.0202	0.0251
4.8	0.0135	0.0167	0.0148	0.0156	0.0146	0.0168	0.0162	0.0210	0.0234
5.0	0.0131	0.0133	0.0141	0.0141	0.0148	0.0159	0.0177	0.0159	0.0206
5.2	0.0123	0.0125	0.0127	0.0119	0.0116	0.0148	0.0146	0.0153	0.0177
5.4	0.0117	0.0122	0.0122	0.0117	0.0119	0.0135	0.0144	0.0146	0.0167
5.6	0.0112	0.0119	0.0104	0.0104	0.0110	0.0122	0.0111	0.0146	0.0156
5.8	0.00893	0.00943	0.0110	0.0110	0.00999	0.0116	0.0139	0.0115	0.0144
6.0	0.00885	0.0106	0.00949	0.00964	0.0103	0.0109	0.00980	0.0125	0.0131
6.2	0.00893	0.0103	0.00906	0.00875	0.00843	0.00997	0.00794	0.00942	0.0122
6.4	0.00911	0.00912	0.00915	0.00817	0.00952	0.00902	0.00923	0.00980	0.0112
6.6	0.00711	0.00802	0.00799	0.00692	0.00834	0.00861	0.00681	0.00936	0.0100
6.8	0.00668	0.00842	0.00748	0.00797	0.00856	0.00819	0.00726	0.00782	0.00881
7.0	0.00671	0.00734	0.00824	0.00748	0.00570	0.00779	0.00812	0.00704	0.00841
7.2	0.00733	0.00656	0.00700	0.00510	0.00751	0.00761	0.00722	0.00836	0.00800
7.4	0.00691	0.00536	0.00659	0.00711	0.00688	0.00710	0.00609	0.00676	0.00801
7.6	0.00619	0.00541	0.00654	0.00631	0.00634	0.00682	0.00663	0.00709	0.00802
7.8	0.00560	0.00529	0.00571	0.00468	0.00605	0.00619	0.00634	0.00601	0.00742
8.0	0.00470	0.00558	0.00505	0.00399	0.00478	0.00556	0.00443	0.00535	0.00681
8.2	0.00462	0.00415	0.00511	0.00374	0.00426	0.00529	0.00538	0.00522	0.00623
8.4	0.00487	0.00462	0.00493	0.00493	0.00468	0.00498	0.00431	0.00526	0.00565
8.6	0.00412	0.00383	0.00427	0.00431	0.00495	0.00467	0.00472	0.00493	0.00533
8.8	0.00454	0.00433	0.00384	0.00417	0.00419	0.00437	0.00449	0.00456	0.00500
9.0	0.00407	0.00436	0.00409	0.00407	0.00365	0.00438	0.00453	0.00444	0.00460
9.2	0.00339	0.00395	0.00364	0.00305	0.00406	0.00439	0.00361	0.00419	0.00419
9.4	0.00320	0.00272	0.00296	0.00364	0.00245	0.00376	0.00328	0.00427	0.00397
9.6	0.00368	0.00240	0.00315	0.00297	0.00333	0.00311	0.00230	0.00298	0.00374
9.8	0.00192	0.00272	0.00267	0.00276	0.00296	0.00264	0.00252	0.00302	0.00274
10.0	0.00231	0.00237	0.00235	0.00192	0.00239	0.00217	0.00169	0.00250	0.00174

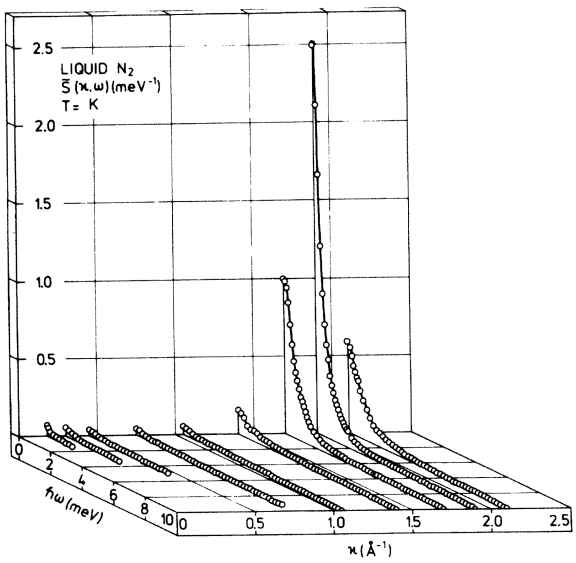

FIG. 5. Perspective view of $\tilde{S}(\kappa,\omega)$.

is the center-of-mass structure factor $S_{\text{c.m.}}(\kappa)$ calculated from the x-ray data for $S(\kappa)$:

$$S(\kappa)=f_1(\kappa)+f_2(\kappa)[S_{\text{c.m.}}(\kappa)-1]\,, \tag{16}$$

with

$$f_1(\kappa)=1+\frac{\sin\kappa d}{\kappa d} \tag{17}$$

and

$$f_2(\kappa)=2\left[\frac{\sin\frac{1}{2}\kappa d^2}{\frac{1}{2}\kappa d}\right], \tag{18}$$

where d is the molecular bond length. Below $S_{\text{c.m.}}(\kappa)$ is of importance in our calculation of $\tilde{S}(\kappa,\omega)$ using the modified Vlasov equation.

B. The moments of $S(\kappa,\omega)$

It is of course of interest to compute the moments of the experimental $S(\kappa,\omega)$ to see how they

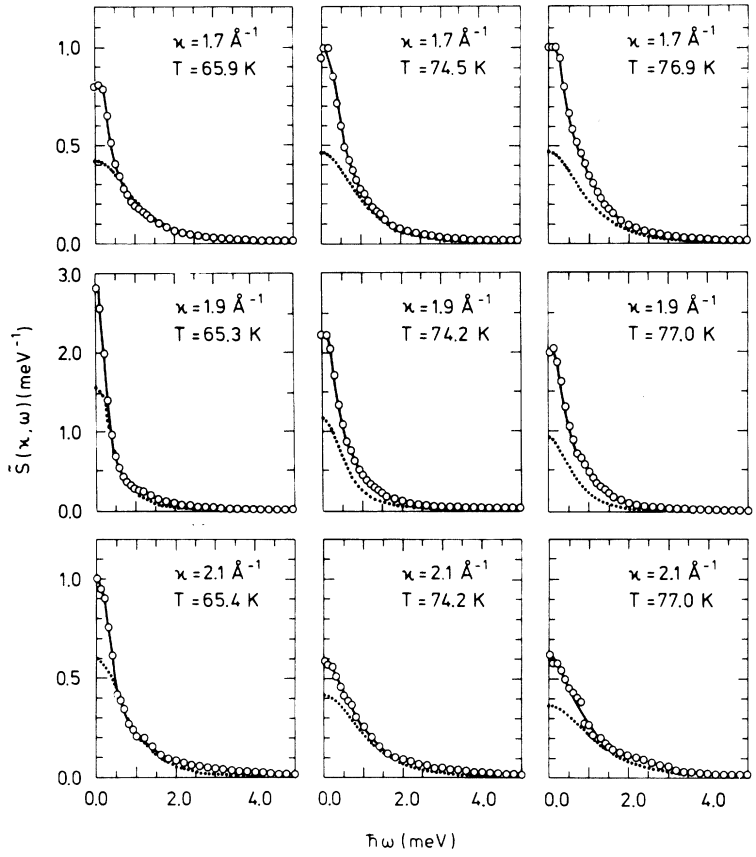

FIG. 6. $\tilde{S}(\kappa,\omega)$ of liquid N_2 determined from neutron inelastic-scattering data (experiment III). The dotted lines represent $\tilde{S}(\kappa,\omega)$ determined from a linearized Vlasov equation.

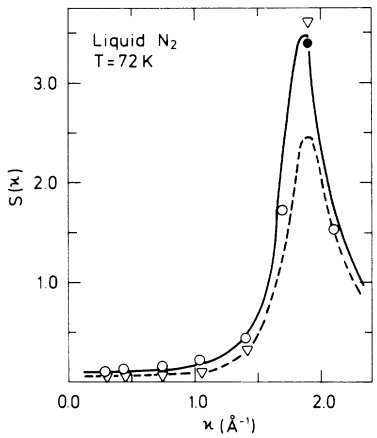

FIG. 7. The static structure factor $S(\kappa)$ of liquid N_2. The line represents the data of Ref. 13 at $T=72$ K. The circles are the values of this work ($T=72$ K). The normalization point is indicated by a full circle. The triangles are values found by a molecular-dynamics simulation at $T=71$ K. The dashed line represents the center-of-mass structure factor $S_{\text{c.m.}}(\kappa)$ calculated from the data of Ref. 13.

agree with (4), (6), and (7). The zeroth moment (4) relates the dynamic structure factor to the static structure factor $S(\kappa)$, and in Fig. 7 we demonstrate that our data are in excellent agreement with $S(\kappa)$ determined by x-ray diffraction. It is worth mentioning that for small wave vectors $S(\kappa)$ assumes the compressibility value of 0.08.

The first frequency moment of $S(\kappa,\omega)$, or the Placzek sum rule, is demonstrated in Fig. 8, where

$$\int_{\Delta E_{\min}}^{\Delta E_{\max}} \hbar\omega S(\kappa,\omega)\, d\hbar\omega$$

is shown versus κ^2. As expected from Eq. (6) we get a straight line, but it should be noticed that the slope corresponds to the mass $M=23.9m_n$, as obtained from a best fit to the data, i.e., close to the molecular mass of N_2. This result is not in contradiction to the earlier results, which indicated that $S(\kappa,\omega)$ was shifted in ω corresponding to the recoil of free nitrogen particles.[3,21] The apparent discrepancy may occur from either the fact that we have taken the first moment of $S(\kappa,\omega)$, whereas

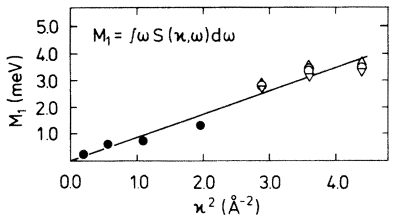

FIG. 8. The 1st-moment sum rule of $S(\kappa,\omega)$ for $T=66$ K (○), $T=72$ K (●), $T=74$ K (▽), and $T=77$ K (△).

the earlier work considered the average frequency, or from the fact that our results are taken at lower κ values. In any case our result is in accordance with the expectation, that for $\kappa \lesssim 2$ Å^{-1}, $S(\kappa,\omega)$ reflects primarily the center of mass dynamics of liquid N_2.

The second frequency moment (7) of the symmetrized dynamic structure factor, $\tilde{S}(\kappa,\omega)$, multiplied by $S(\kappa)/[\frac{5}{6}+m(\xi)]$ is shown versus κ^2 in Fig. 9. Here the best-fitted slope corresponds to a nominal mass of $14.4m_n$, i.e., close to the atomic mass. It is to our knowledge the first time the "de Gennes sum rule" (7) has been demonstrated experimentally for a diatomic liquid.

VI. DISCUSSION AND CONCLUSIONS

The experimentally determined dynamic structure factor, $S(\kappa,\omega)$, covers the wave vectors from the collective (or small-κ) region to the single particle (or large-κ) region. As mentioned above, in the region 0.3 Å$^{-1} \leq \kappa \leq 1.9$ Å^{-1}, $S(\kappa,\omega)$ was derived by computer simulation and we have chosen wave vectors close to those of this study in order to facilitate comparison. Apart from such a comparison, we discuss below our results in the light of two relevant theories, covering opposite κ regions.

The linear hydrodynamic theory of fluids accounts in general very well for experimental results

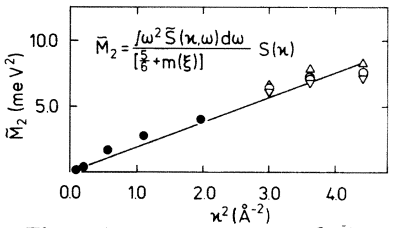

FIG. 9. The 2nd-moment sum rule of $\tilde{S}(\kappa,\omega)$ for $T=66$ K (○), $T=72$ K (●), $T=74$ K (▽), and $T=77$ K (△).

at small wave vectors, i.e., when wavelengths are large compared to intermolecular distances. Above we used the hydrodynamic results (9) for $\tilde{S}(\kappa,\omega)$ in connection with the multiple-scattering corrections. These corrections do not depend on the details of the structure factor, so that deviations between the measured $S(\kappa,\omega)$ and (9) do not influence our final result. It is therefore relevant to compare $\tilde{S}(\kappa,\omega)$ to (9) to investigate how well the hydrodynamic continuum theory applies at wavelengths as short as 20 Å, i.e., quite close to the intermolecular distances in the liquid. In Fig. 10 we show this comparison for wave vectors from 0.18 Å^{-1} to 0.3 Å^{-1}. Figure 10 demonstrates that hydrodynamic theory accounts relatively well for the experimental structure factor, although it shows less broadening of both the central Rayleigh line and of the Brillouin lines. In order to investigate this more quantitively, we have fitted the measured $\tilde{S}(\kappa,\omega)$ to the hydrodynamic line shape

$$\tilde{S}(\kappa,\omega)=\frac{A_0}{\pi}\frac{\Gamma_0}{\omega^2+\Gamma_0^2}+\frac{A_1}{\pi}\frac{\Gamma_1}{(\omega-\Omega_1)^2+\Gamma_1^2}\ . \tag{19}$$

Comparing (19) to (9) and (10), hydrodynamic theory predicts the following relations:

$$\begin{aligned} &A_0+2A_1=k_BT/(Mc_S^2)\ , \\ &2A_1/A_0=\gamma-1\ , \\ &\Gamma_0=D_T\kappa^2\ , \\ &\Omega_1=c_S\kappa\ , \end{aligned} \tag{20}$$

and

$$\Gamma_1=\Gamma\kappa^2\ .$$

Figure 11 shows the results of the fit compared to the results of the theory when using the num-

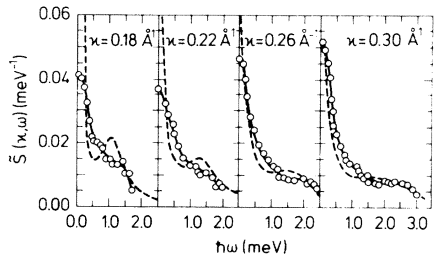

FIG. 10. Dynamic structure factors $\tilde{S}(\kappa,\omega)$ of liquid N_2 determined from neutron inelastic-scattering data (experiment II) at $T=74$ K. The dashed lines represent the $S(\kappa,\omega)$ obtained from hydrodynamic theory.

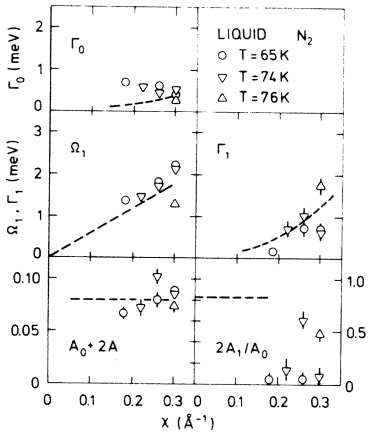

FIG. 11. Line-shape analysis of $\tilde{S}(\kappa,\omega)$ according to hydrodynamic theory. The dashed lines are extrapolations of the theory with parameters taken from transport measurements (at $\kappa \approx 0$).

bers for c_S, Γ, and D_T given above. It shows that hydrodynamic theory accounts quantitatively for the observed Brillouin line parameters c_S and Γ, as well as for the integrated intensity $S(\kappa)$. The thermal diffusivity D_T is not well reproduced. This could be related to the problem of finite κ resolution, which may have a broadening effect on the experimental $S(\kappa,\omega)$. The odd behavior of Γ_0 vs κ points towards the same deficiencies in the data. Finally, the specific heat ratio $C_p/C_v = 2A_1/A_0 + 1$ is derived to be quite small, but the significance of this observation is not quite clear in the light of the problems with the central part of our $S(\kappa,\omega)$. The composite evidence is that hydrodynamic theory explains our measured $S(\kappa,\omega)$ well even at the very short wavelengths considered. In particular, Figs. 10 and 11 indicate that at $\kappa = 0.3$ Å^{-1} the agreement is quantitative.

Secondly, it is interesting to compare our results with those of the molecular-dynamics calculation by Weis and Levesque in the wave-vector region 0.3 Å$^{-1} \leq \kappa \leq 1.9$ Å^{-1}. This is done in Fig. 12. However, the comparison is complicated by the fact that $S(\kappa)$ in the calculation is appreciably less than the well-established experimental value except when $\kappa = 1.9$ Å^{-1}. We have therefore chosen to compare our $S(\kappa,\omega)$ both to the absolute values given in Ref. 4, as well as to the relative values by adjusting $S(\kappa,0)$. Apart from when $\kappa \approx 1.9$ Å^{-1} there are important differences between the calculated $S(\kappa,\omega)$ and the measured one in Fig. 12. At $\kappa = 0.30$ Å^{-1}, where the neutron results agree qualitatively with the hydrodynamic theory, molecular dynamics shows a well-resolved side peak, indicating a sound velocity of almost twice the hydrodynamic value. However, the widths of the lines agree rather well with the neutron results as well as with hydrodynamics. This is true both for the central line, where the width is determined by thermal diffusivity D_T, and for the Brillouin line where the width stems from the finite lifetimes of

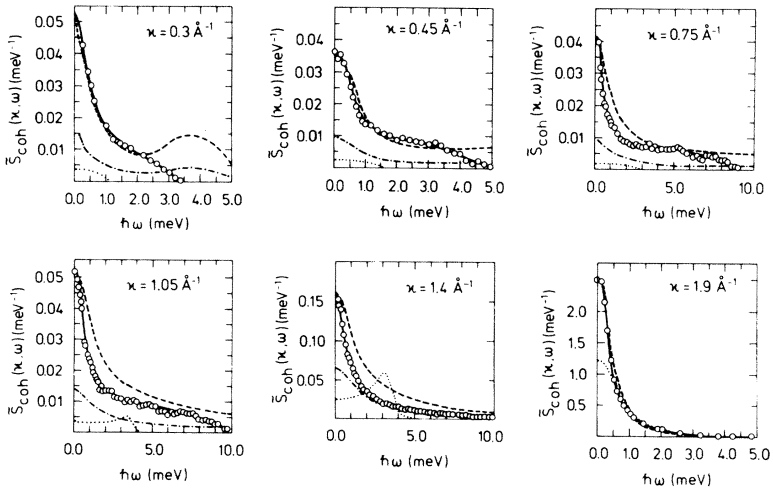

FIG. 12. Dynamic structure factors $\tilde{S}(\kappa,\omega)$ of liquid N_2 determined from neutron inelastic-scattering data at $T = 72$ K (experiment I) and by molecular dynamics simulation at $T = 71$ K. The MD data are shown normalized to the same $\tilde{S}(\kappa,0)$ as the experimentally determined $\tilde{S}(\kappa,0)$ (- - -) and applying the $S(\kappa)$ value determined by the MD simulation (- · - ·). The line (· · · ·) represents the $\tilde{S}(\kappa,\omega)$ determined from a linearized Vlasov equation ($T = 72$ K).

the sound waves, as given by Γ. As κ increases there is in both the experimental and the computed $S(\kappa,\omega)$ an increasing smearing and merging of the two lines, but the trend is the same as when $\kappa=0.3$ Å^{-1}. The results are in reasonable agreement as regards the central peak, but the computed line shape extends far out in ω. Only at 1.9 Å^{-1} do the two results coalesce at all frequencies. The comparison therefore indicates that the compressibility or inverse sound velocity of the computer liquid is underestimated but that relaxation processes are well accounted for in the calculation. It should of course be noted that an underestimated compressibility in the computer liquid decreases $S(\kappa)$ in the compressibility region (10). This is indeed observable in Fig. 7 where the static structure factors are shown. Here the computed $S(\kappa)$ approaches a value which is about one-third of the correct value. Literally we find from both $S(\kappa,\omega)$ and from $S(\kappa)$ that molecular dynamics implies a sound velocity of $1.7c_S$, a strong indication that our consistent analysis of the deficiencies in the computer liquid is correct.

Figure 11 also compares our results with a modification of the theory presented by Singwi *et al.*[22] for the collective motions. It is based on a linearized Vlasov equation[23] and claimed to be valid at short wavelengths and high frequencies. The dynamic structure factor is predicted from the static structure factor, $S(\kappa)$. We have applied this theory to liquid N_2. Because N_2 consists of diatomic molecules, the calculations turned out to be more complicated than in the atomic case. To get through to an expression for $S(\kappa,\omega)$ we had to restrict the calculations to center-of-mass motions. We then obtained the following expression:

$$S(\vec{\kappa},\omega)=\frac{\frac{1}{\sqrt{\pi}\omega_0}\exp\left[-\frac{\omega^2}{\omega_0^2}\right]}{\left[\frac{1}{S_{\text{c.m.}}(\vec{\kappa})}-\frac{1-S_{\text{c.m.}}(\vec{\kappa})}{S_{\text{c.m.}}(\vec{\kappa})}\frac{2\omega}{\omega_0}\exp\left[-\frac{\omega^2}{\omega_0^2}\right]\int_0^{\omega/\omega_0}\exp(t^2)\,dt\right]^2+\left[\frac{1-S_{\text{c.m.}}(\vec{\kappa})}{S_{\text{c.m.}}(\vec{\kappa})}\frac{\sqrt{\pi}\omega}{\omega_0}\exp\left[-\frac{\omega^2}{\omega_0^2}\right]\right]^2} \tag{21}$$

where

$$\omega_0=\frac{(2k_BT\vec{\kappa}^2)^{1/2}}{M}\,. \tag{22}$$

For κ values below 1.7 Å^{-1} the agreement with both experimental data and MD data is very bad. At $\kappa=1.05$ Å^{-1} and $\kappa=1.40$ Å^{-1} the calculated dynamic structure factors have a well-defined side peak at $\hbar\omega\approx 3$ meV. It is in agreement with what is found by Nelkin *et al.*[24] applying a linearized Vlasov equation to a classical liquid, but as is apparent from Fig. 10 it is not confirmed by the experiments. For $\kappa\geq 1.7$ Å^{-1} and $\hbar\omega\gtrsim 0.5$ meV there is a reasonable agreement between the dynamic structure factors predicted by the theory and those determined from the experimental data. Furthermore it is noteworthy that the theory predicts the general trends of the effect of varying the temperature, i.e., whether the heights and widths of the central peaks are increased or decreased with temperature. This is demonstrated in Fig. 6, where we compare the temperature dependence of $S(\kappa,\omega)$ at $\kappa\approx 1.9$ Å^{-1} to that of Eq. (21) for these temperatures. Thus the noticeable temperature dependence in liquid nitrogen at wave vectors around the peak in $S(\kappa)$ can be understood in the basis of the modified Vlasov equation.

ACKNOWLEDGMENT

We wish to thank the Danish Natural Science Research Council for sponsoring the computer calculations.

*Present address: Instituttet for Kemiteknik, The Technical University of Denmark, DK-2800 Lyngby.

[1]J. C. Dore, G. Walford, and D. I. Page, Mol. Phys. 29, 565 (1975).

[2]K. S. Pedersen, F. Y. Hansen, and K. Carneiro, J. Chem. Phys. 70, 1051 (1979).

[3]K. Carneiro and J. P. McTague, Phys. Rev. A 11, 1744 (1975).

[4]J. J. Weis and D. Levesque, Phys. Rev. A 13, 450 (1976).
[5]J. R. D. Copley, Comput. Phys. Commun. 7, 289 (1974).
[6]V. F. Sears, Adv. Phys. 24, 1 (1975).
[7]P. Schofield, Phys. Rev. Lett. 4, 239 (1960).
[8]G. Placzek, Phys. Rev. 86, 377 (1952).
[9]P. G. de Gennes, Physica 25, 825 (1959).
[10]G. Dolling and V. F. Sears, Nucl. Instrum. Methods 106, 419 (1973).
[11]K. Sköld, J. M. Rowe, G. Ostrowski, and P. D. Randolph, Phys. Rev. A 6, 1107 (1972).
[12]J. R. D. Copley and J. M. Rowe, Phys. Rev. A 9, 1656 (1974).
[13]A. W. Furumuto and C. W. Shaw, Phys. Fluids 7, 1026 (1974); tabulated by P. W. Schmidt and C. W. Tompson in Ref. 15.
[14]J. P. Hansen and I. R. McDonald, *Theory of Simple Liquids* (Academic, London, 1976).
[15]H. L. Frisch and Z. W. Salsburg, *Simple Dense Fluids* (Academic, New York, 1968).
[16]See, for example, W. Marshall and S. W. Lovesey, *Theory of Thermal Neutron Scattering* (Oxford University Press, Oxford, 1971).
[17]R. G. Sachs and E. Teller, Phys. Rev. 60, 18 (1941).
[18]J. G. Powles, Adv. Phys. 22, 1 (1973).
[19]B. T. M. Willis, *Chemical Application of Thermal Neutron Scattering* (Clarendon, Oxford, 1972), Appendix I.
[20]J. Barojas, D. Levesque, and B. Quentrec, Phys. Rev. A 7, 1092 (1973).
[21]R. N. Sinclair, J. H. Clarke, and J. C. Dore, J. Phys. C 8, L41 (1975).
[22]K. S. Singwi, K. Sköld, and M. P. Tosi, Phys. Rev. A 1, 454 (1970).
[23]A. A. Vlasov, *Many Particle Theory and its Application to Plasmas* (Gordon and Breach, New York, 1961).
[24]M. Nelkin and S. Ranganathan, Phys. Rev. 164, 222 (1967).